

Field measurements in river embankments: validation and management with spatial database and webGIS

Lucia Simeoni · Paolo Zatelli · Claudio Floretta

Received: 18 December 2012 / Accepted: 11 November 2013 / Published online: 20 November 2013
© Springer Science+Business Media Dordrecht 2013

Abstract This study focuses on the development of a system with a spatial database and a webGIS able to store, validate and display the data to assist the decision makers in managing early warning systems for river embankment failure. In order to obtain precise results, it is essential to have a tool with ability of managing a large number of data for checking their reliability and for locating them in the space. In this paper, special emphasis was given in the development of procedures to assess the reliability of the measures. For this purpose, the database includes all the information needed to describe the instrument performance, such as the sand pack size and casing diameter of open-standpipe piezometers for evaluating their time lag, and the calibration curves of transducers with the possibility of their updating. The position of the non-functioning instruments is identified through the analysis of the electrical signal and spatial displays, while the analyses of the redundancy and coherence of measures is used for detecting doubtful data. Database and webGIS were applied to the monitoring data of an embankment of the Adige River in Northern Italy. The database and webGIS system has proved to be a suitable and effective tool for the management and validation of real-time data and periodical field measurements.

Keywords River embankment · Failure · Field measurements · Spatial database · webGIS · Data validation

L. Simeoni (✉) · P. Zatelli · C. Floretta
Department of Civil, Environmental and Mechanical Engineering, University of Trento,
Via Mesiano 77, 38123 Trento, Italy
e-mail: lucia.simeoni@univaq.it

Present Address:

L. Simeoni
Department of Civil, Construction-Architectural and Environmental Engineering,
University of L'Aquila, Via Giovanni Gronchi 18, Zona industriale di Pile, 67100 L'Aquila, Italy

1 Introduction

River embankments are geotechnical structures that may fail in preventing flooding due to the water overtopping, but also due to inner (river side) or outer (land side) slope failure, as well as piping or uplift. Overtopping is the major mode of failure for modern well-kept fluvial dikes (Merz 2006), where the seepage can be efficiently controlled by drains or impervious materials, but for older historically grown dikes without drainage the consideration of the other mechanisms is required. In the older dikes, the embankment crest usually exceeds the design water river level by an appropriate freeboard, calculated with reference to a return period, with the consequence that the probability of overtopping is normally smaller than the frequency of failure due to the geometrical and geotechnical conditions. The comprehension of failure modes is therefore fundamental for the flood risk assessment, but it may be a difficult task due to the complexity of the flood defense structures, and only the detailed studies supported by field measurements could provide a reliable knowledge of the failure mechanisms (Morris et al. 2009).

The complexity mainly derives from the natural and hand-made heterogeneity of the soils. Soils underlying the embankments naturally present heterogeneity at various scales of description due to different depositional conditions and different loading histories (Elkateb et al. 2003). In addition, embankments are not homogenous if different soils have been used for the core and lateral berms. The soil spatial variability may influence the stability of embankments, especially by affecting the seepage and, therefore, the pore-water pressure distribution. Uncertainties due to the variability presumably are taken into account indirectly for design purposes by selecting a factor of safety, which is chosen on experience and/or some design criteria. Alternatively, reliability analyses should be carried out if a better knowledge of the effects of the variability on the stability of embankments is desired. For example, introducing uncertainties in terms of statistical variables (i.e., through mean, variance, coefficient of skewness, probability density functions and cumulative density functions), Christian et al. (1994) suggested to use the reliability index instead of the factor of safety F_s , since it describes the number of standard deviations (i.e., the amount of uncertainty in the calculated value of F_s) separating the best estimate of F_s from its defined failure value of 1.0. The authors also found that uncertainty in the values of the soil properties is a major contributor to the uncertainty in the stability of the embankments. Similar results were obtained by Van Der Most and Wehrung (2005) for flood defense structures in the Netherlands, where adequate information on subsoil and inner material of dikes as well as on the foundation of hydraulic structures is lacking in quite a few cases. This lack of information introduces knowledge uncertainties in the decision-making process with the consequence that the reliability of the calculated flood risk may be low, and it could be increased through further research. Also Vorogushyn et al. (2009) developed the fragility functions for describing the probability of failure of a dike section due to piping and micro-instability and found that the probability of breaching is conditioned by the uncertainty in geometrical and geotechnical dike parameters. The sensitivity analysis identified a particularly strong dependence of the seepage fragility function and the fragility function for critical pipe development to the mean hydraulic conductivity of the dike core and the foundation materials. Great influence of the hydraulic conductivity on the flow patterns and stability of embankments was also found by Cho (2012) and Gui et al. (2000).

In addition to those related to the characteristics of the soils, Vrijling (2001) specified that the uncertainties to be taken into account in a reliability analysis of flooding prediction are intrinsic of the natural phenomenon (i.e., the extreme river discharges), and also reside

in the engineering models that could not predict correctly the behavior of river courses, dikes and structures.

Field measurements provide a fundamental contribution for the comprehension of the flood structures behavior and consequently for a better knowledge of the failure mechanism that is more likely to occur. It is known that failure is always caused by an increase in pore-water pressure that reduces the soil shear strength, independent of the type of mechanism among inner or outer slope failure, piping or uplift. What changes from a type of mechanism to another one is the pore-water pressure distribution over time (Marsland and Randolph 1978; Staiano et al. 2001; Van Beek et al. 2010). For this purpose, piezometers are commonly used to monitor the pore-water pressure for defining the boundary conditions in seepage analyses, to estimate the model parameters (mainly the hydraulic conductivities of soils) or to verify the analyses results.

Since pore-water pressure may change rapidly, especially in piping phenomena (Van Beek et al. 2010), as well as varying at different rate due to a transient condition occurring also after the peak flood (Oka et al. 2008, Staiano et al. 2001), measurements should be collected automatically at least at hourly frequencies. Real-time monitoring should also be available if it is included in an early warning system (EWS) (Gallace and Uchimura 2010), which use is increasing thanks to the development of information and communication technologies (ICT) (Hopman et al. 2011). The EWSs make the river embankments safer (Meijer and Koelewijn 2008) when their stability is evaluated in real time, but require an effective tool for collecting, managing and analyzing a large amount of geospatial and temporal data, such as ground surface, geology, hydraulic and mechanical soil characteristics, water level in the river, groundwater pressure, surface and soil displacements, meteorology, etc.

This study focuses on the development of a spatial database and a webGIS able to store, validate and display the data to assist decision makers in managing an EWS. By developing a sensor observation service (SOS), the database could be linked to the sensors (including geospatial data and manual measurements), and the webGIS could interact with users for displaying the data and collecting more additional information.

The database was set up by using PostgreSQL and PostGIS; the webGIS displays the data. Special attention was paid to the development of data validation procedures to assess the reliability of the measurements. For this purpose, the database includes all the information needed to describe the instrument performance, such as the sand pack size and casing diameter of open-standpipe piezometers for evaluating their time lag, and the calibration curves of transducers with the possibility of their updating. The position of the non-functioning instruments is identified through the analysis of the electrical signal and spatial displays, while the analyses of the redundancy and coherence of measures are used for detecting doubtful data.

An example of application of database and webGIS is given for the field measurements at an embankment of the Adige River in Northern Italy. Measurements of groundwater pressure, soil vertical displacements, soil and instrument temperatures, meteorology and water level of the river were processed.

2 Reliability of measurements: accuracy and data validation

Field measurements must be used in geotechnical problems only after their reliability has been assessed. Reliability of measurements is paramount in any monitoring system, and particularly in an EWS (DiBiagio and Kjekstad 2007), whose success depends on its ability to identify and measure small but significant indicators that precede the failure. Since the

warning involves the community living close to the structure likely to fail, the community should be confident that a structure with an EWS is a safer structure (Meijer and Koelewijn 2008) and any data processing able to avoid false alarms should be carried out. Measurements are reliable if they are available at any time (i.e., continuous data collection) and if they are accurate.

The accuracy of measurements relies on the capability of the monitoring system to provide the closest possible value to the true value of the quantity measured (Dunncliff 1993). The value of the quantity present in the soil without the instrument is referred to as the true value. Accuracy mainly depends on the instrument conformance, on the calibration curve and on the influence of the environmental factors, such as the temperature. In turn, given the instrument, its conformance depends also on the type of installation since the conformance is the capability of the instrument to not alter the true value.

Redundancy and alternative measurement methods should be considered in order to assess the reliability of field measurements. Accordingly, the data validation may be carried out in terms of redundancy of measurements, by comparing measurements of the same type, and of coherence, by comparing measurements describing the same physical phenomenon.

In conclusion, a data management system for the reliability assessment of field measurements should include: information about the installation for evaluating the instrument conformance, information on the environmental conditions, checking procedures to verify the data acquisition and the instrument calibration, data processing for their validation in terms of redundancy and coherence.

The field measurements cannot solve automatically a geotechnical problem because it is likely that instrumentation does not measure phenomena occurring outside the instrumented area or at a level too low to be measured. In effect, Professor Ralph Peck pointed out that visual observations made by an intelligent human being remain one of the most powerful instruments (NGI 2000), and accordingly the monitoring systems are including more and more often technologies such as powerful digital cameras (Marr 2013). Thus, the data management system must include tools for data visualization, such as maps, tables, graphs, for providing information that helps the decision makers to interpret the phenomena, rather than to give automatically orders or alarms. The database management system coupled with the webGIS has resulted to be an effective solution for managing monitoring data and spatial information, especially to storage and display the data (Yoo and Kim 2007; Huang et al. 2005). Even though it has also been used to assist the decision makers in managing EWSs (Crossland et al. 1995; Fan-Chieh et al. 2007), not enough emphasis on the assessment of the reliability of measurements it has been given.

3 The spatial database and webGIS system

The system collects a large quantity of heterogeneous data which can, directly or indirectly, be linked to a geographic location; therefore, a database management system (DBMS) able to deal with geographic data and offering function to process geometry and topology has been used.

While system maintainers are usually comfortable with accessing directly the database through specialized tools, system users must be able to access all the system's functions using an intuitive interface, possibly in a networked environment, which presents the information as tables, graphs and maps. For this reason, a webGIS provides the interface for the users.

The implementation follows the open geospatial consortium (2010) standards using free and open source software (FOSS), which makes possible its customization and modification and to redistribute the whole system.

The system is based on custom developments of PostgreSQL (2010), as DBMS, with the PostGIS (2010) spatial extension and Geoserver as webGIS.

The spatial database is divided into two schemas: one for the data which are supposed to be constant or seldom change and one for the variable data. The first scheme contains tables describing instruments, their location and calibration data, the second scheme contains tables for the measurements and their metadata (such as collecting date, file names, etc.).

The user accesses the system through the webGIS interface for browsing the available data and uploading new measurements and the calibration curves.

The information is presented to the user as customizable tables, graphs and maps, representing instruments' status and their location. It is also possible to view cross sections, where displacement values and their position with respect to a warning threshold are shown.

Special graphs (Fig. 12) are used to display the instruments' operational state during a time span.

The webGIS server side uses Apache 2.0 (2010) as web server and Geoserver (2010) as a WMS/WFS server following OGC's standard for raster and vector maps. Dynamic charts are created using the Open Flash Chart PHP library (2010). The Keyhole Markup Language (KML) is used for the PopUp windows describing the instruments or their current operational status.

The client side is written in the JavaScript language and uses the MapFISH framework (2010), combining OpenLayers (2010) and ExtJS (2010), and it is locally executed by the browser without the need to install any software.

Both the server and the client parts have been customized, with the creation of new JavaScript and PHP scripts.

This approach has the advantage of allowing the remote access through the web using a standard web browser client, while providing easy, fast and real-time visualization of large datasets and immediate visual assessment of the current operational status of the system.

4 Adige River embankment hazards

The lower Adige Valley, located South of Bolzano in Northern Italy (Fig. 1), is a "classic" glacial valley with straight and smooth walls and a flat base. The resulting gentle slope allowed the Adige River to develop a sinuous meander pattern across the broad flood plain. Until the middle of the nineteenth century, the low-gradient, meandering Adige River was particularly susceptible to over-bank flow during high water, and its flood plain was subjected to periodic flooding. In order to prevent this flooding and to facilitate the design and construction of the Verona-Brennero railway, in the periods 1817–1826 and 1879–1885, the natural path of the river was straightened by building embankments (Fig. 2) with the consequence that currently the river is trained between these levees and cannot form new meanders.

The river embankments are about 7 m height; they are generally made of coarse-grained well-graded soils, but locally may include layers of finer materials. The soil profile at different sections of the embankment is extremely variable because the Adige River had a braided form. Consequently, when dealing with the stability analyses, the soil profile varies

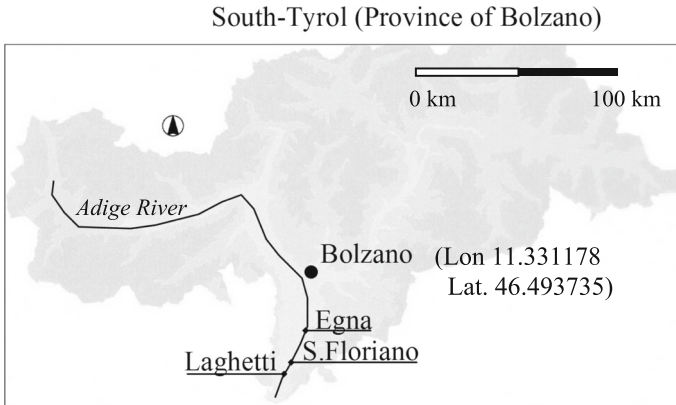


Fig. 1 The Adige River in the Autonomous Province of Bolzano-Bozen

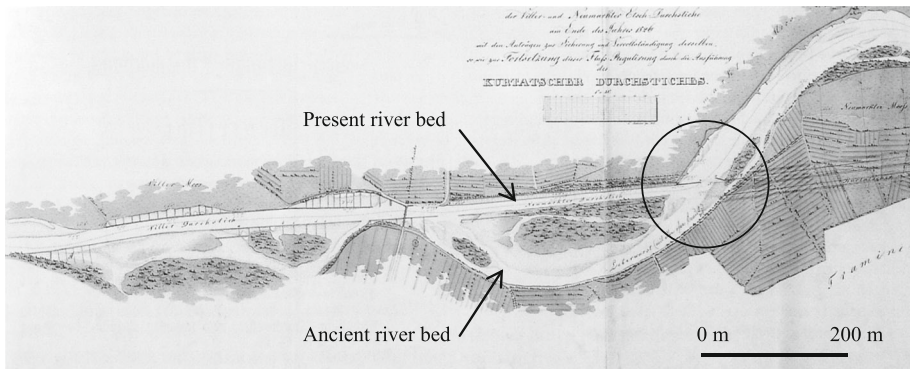


Fig. 2 Rectification of the Adige river (flowing from right to left) near Egna from a 1826 plan: the circle includes the studied area (Werth 2003 modified)

at any cross section, and the associated heterogeneity and the anisotropy of the hydraulic conductivity influence the mechanism of failure.

Since the river rectification occasional failures have occurred, with the most dangerous in 1981 when a breach formed at an intersection between the present and the ancient river bed (at Laghetti in Fig. 1), and more than 3 m of water flooded the near village of Salorno. The need to assess the hazards related to the stability of the embankments was therefore recognized, and to this end, the stability conditions of a case of intersection located at Egna, 20 km south of Bolzano was studied. The study included field measurements aimed at collecting the information necessary to define the pore-water pressure distribution and the displacements of the embankment and its foundation.

5 The case study of Egna

A reach of the right-hand embankment of the Adige River at Egna, where the present river intersects the ancient bed (Fig. 2), was selected for studying its stability and the settlements that it was suspected have occurred since the construction of the embankments.

As seen in Fig. 3, a failure of this embankment would cause the flooding of apple orchards, factories, houses and two important sections of transport infrastructure connecting Italy to the Northern Europe: the Verona-Brennero railway and the Modena-Brennero motorway. The study was based on field measurements collected on three sections: A, B, C, with B the main section and A and C the secondary ones. Figure 4 shows the soil profiles and the installed instrumentation. Embankment (A1, A2 and A3) is a quite homogenous gravel with silty sand; the ancient river bed (B) has a similar grain size, but it is more heterogeneous; the soil C is an extremely heterogeneous fluvio-lacustrine deposit: C1 and C3 vary from silty sand to gravel with silty sand, the finer C2 varies from silt with clay to slightly clayey silt. Significant layers of peat were identified in the section B between soil B and C1, and in soil C2 at an elevation of 192 m.

According to Dunnycliff (1993), the preliminary action prior to planning a monitoring system was the identification of the specific geotechnical problems, followed by the definition of mechanisms and phenomena that should be investigated (Table 1). Every instrument was therefore selected to assist in answering a specific question arising from two problems: the stability of the embankment and the settlement of the soil foundation. The stability was supposed to rely mainly on the pore-water pressure changes, with mechanisms of inner or outer slope failure, as well as uplift or pipe phenomena. Then, many instruments were installed for analyzing the seepage (Pozzato 2009) and for giving a significant contribution to the knowledge of seepage models as suggested by Morris et al. (2009).

In the secondary sections A and C, two nested piezometers were installed on both inner ($p1$) and outer ($p2$) sides of the embankment. In each vertical profile, three filter tips (a , b and c) were installed using sand packs and bentonite sealing; for automatic collection of data the deepest ones (b and c), lying below the water table, were equipped with pressure transducers plugging the top of the filter tips. In the main section B, the instrumentation consisted of: three nested piezometers ($p1$ and $p2$ on the embankment sides, $p3$ distant in the orchards, where a sand crater formed in the past), three multipoint extensometers (mx , steel rods and packer anchors), with two bases (a and b) on the embankment sides and three (a , b and c) in the center, collecting automatic measurements by potentiometer displacement transducers, two extensor-inclinometers TRIVEC (T1, in the center close to BMX2, and T2, in the outer side close to BMX3), four water content probes, 3 geothermometers, one meteorological station. Details of the monitoring system are given in Simeoni et al. (2008). The automatic measurements have been collected at a time interval of 15 min and downloaded via FTP, but the necessity was soon recognized of using a data management tool for handling the data monitoring. A system of a spatial database with a webGIS was identified as the most effective tool for collecting, storing, mapping, displaying and validating the measurements.

So far, the monitoring was aimed at providing information to define the possible failure mechanisms by means of seepage and slope stability back-analyses (scientific aim of the monitoring: Pozzato 2009). In this phase the webGIS is an effective tool:

- to collect, store and display in real-time data provided by different instruments;
- to share the information with users located at different sites (for this case study, mainly at the University of Trento and at the Province of Bolzano);
- to implement procedures for checking the performance of the instruments;
- to implement procedures for validating the data.

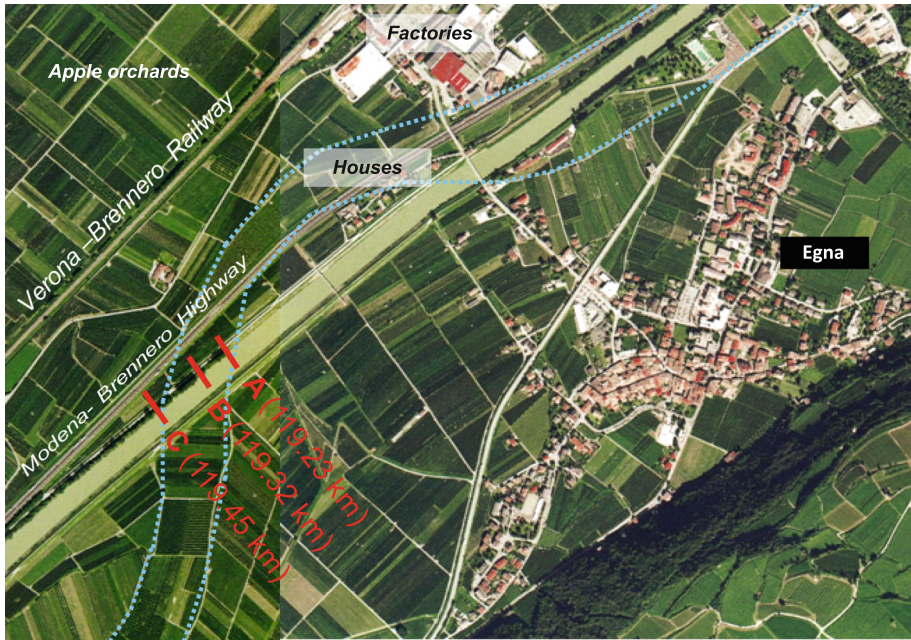


Fig. 3 Location of the case study at Egna. Three sections *A*, *B* and *C* were monitored at the intersection between the present and ancient river bed

When the failure mechanism has been identified, the monitoring may then be used for the real-time evaluation of hazards in EWSs (Civil Defense aim of the monitoring), and the webGIS is also an effective tool for:

- the real-time evaluation of hazards

by defining a web processing service (WPS) and a sensor observation service (SOS) including a sensor alert service (SAS).

To satisfy both requirements, it was necessary to use simple instrumentation that could be easily and extensively installed along the river embankments, while at the same time providing sufficiently precise and accurate data as required by the scientific project. Great attention was therefore paid in evaluating the accuracy and reliability of measurements (Simeoni et al. 2008). Figure 5 shows the workflow followed for identifying and computing for each part of the monitoring system the errors affecting the accuracy of measurements, as well as the data processing used for validating them. In the following, the GIS-based tool setups for piezometers and extensometers are described.

6 GIS-based tools for managing the accuracy of measurements

Accuracy resulting from errors due to instrument conformance, improper calibration and temperature effects was analyzed by developing a pertinent data processing.

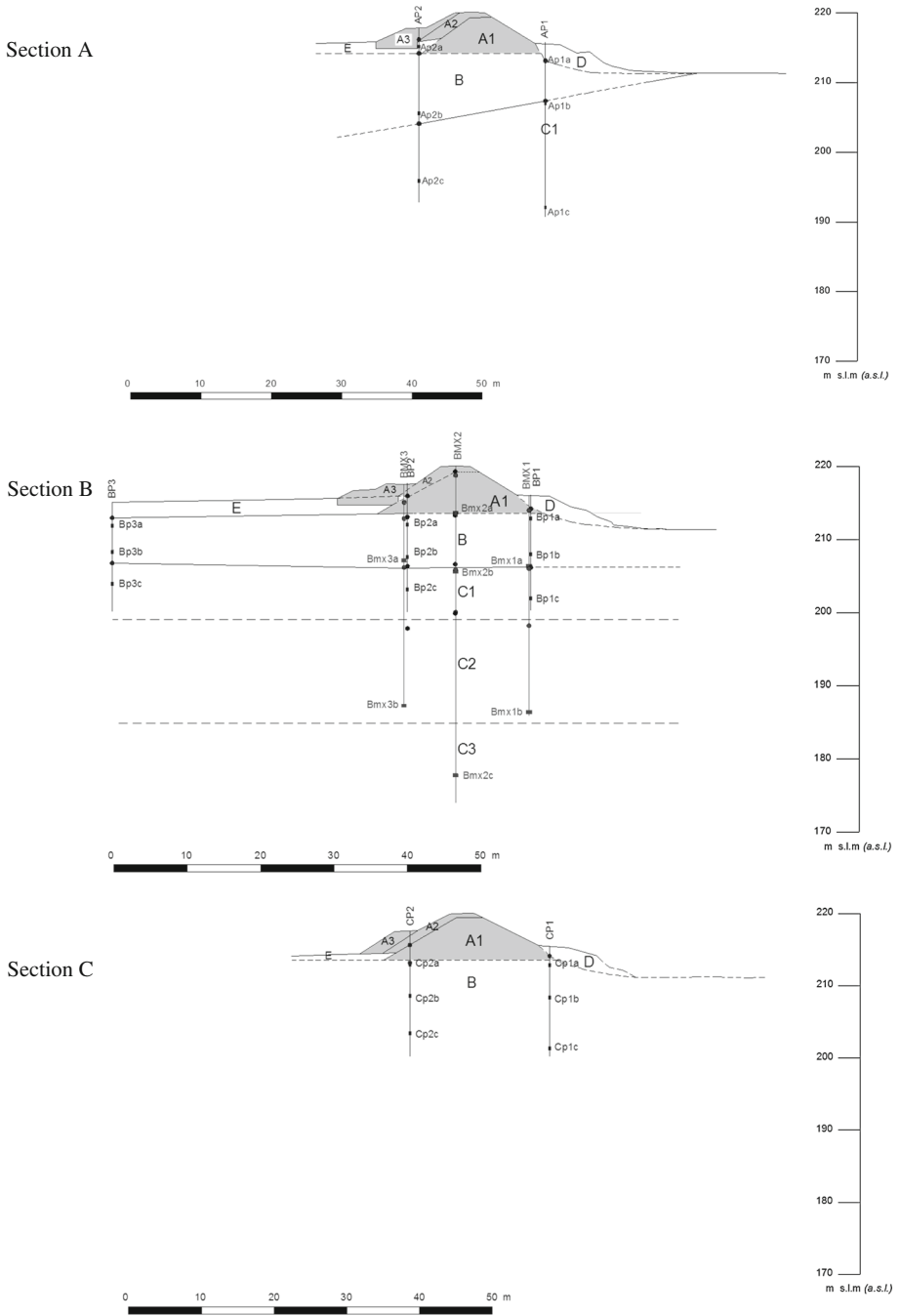


Fig. 4 Monitored sections: soil profile (A1, A2, A3 = embankment; B = ancient river bed; C1, C2, C3 = fluvio-lacustrine deposit; D = fluvial sediments; E = agricultural soil) and instrument location (P = piezometer; MX = multipoint extensometer); T = TRIVEC)

Table 1 From problem to instrumentation

Problem	Mechanism	Phenomenon to be described (<i>physical quantity to be measured</i>)	Instrumentation
Stability of the embankment	<ol style="list-style-type: none"> 1. Shear strength reduction due to (positive) pore pressure increase and suction reduction 2. Shear strength reduction due to strong upward hydraulic gradients (piping) 	<ol style="list-style-type: none"> 1. Seepage and infiltration (<i>pore pressure or total head below water table; water content above water table; boundary conditions: river level, rainfall, air temperature, wind, relative humidity, radiation, air pressure, soil temperature</i>) 2. Displacement evolution (<i>horizontal and vertical displacements</i>) 3. Vertical displacement evolution (<i>vertical displacements</i>) 	<ol style="list-style-type: none"> 21 Piezometers (A/M) 4 Environsmart (A) 1 Meteorological station (A) 3 Geothermometers (A) 9 Extensometers (A/M) 2 Inclinometers (M)
Settlement	<ol style="list-style-type: none"> 3. Secondary consolidation 	<ol style="list-style-type: none"> 3. Vertical displacement evolution (<i>vertical displacements</i>) 	<ol style="list-style-type: none"> 9 Extensometers (A/M)

(A) = automatic measurement; (M) = manual measurement

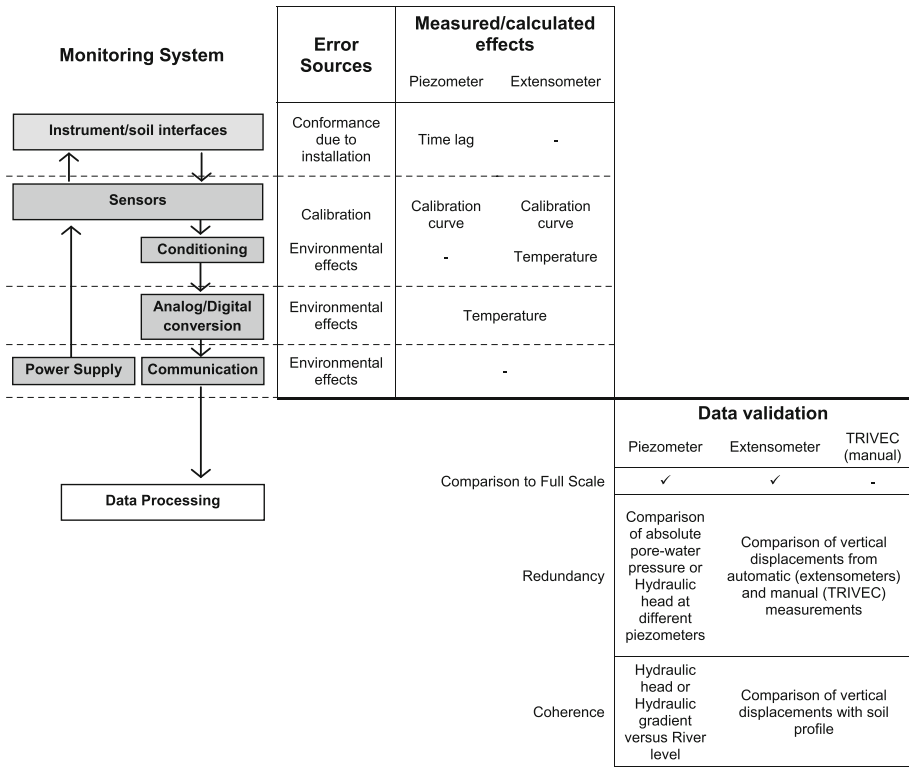


Fig. 5 Workflow for controlling the sources of errors and for the data validation

6.1 Instrument conformance of piezometers and extensometers

Piezometers with open standpipes, filter tips, fine gravel filters and bentonite sealings (Fig. 6) were used. Conformance of piezometers is therefore related to the effectiveness of the bentonite sealings to avoid any vertical seepage around the pipes (Vaughan 1969), and to the time lag. Assuming the volume deformation of the soil skeleton is negligible, for open-standpipe piezometers, the time lag depends on the permeability of the soil and on the geometrical entities related to the shape of the pipe and of the intake filter (Hvorslev 1951):

$$t_{95} = - \frac{A}{F \cdot k_h} \ln 0.05 \tag{1}$$

where t_{95} is the time needed to reach the 95 % of the water level at equilibrium, A is the cross-sectional area of the pipe, F the intake factor depending on length L and diameter D of the filter and on the ratio between the horizontal and vertical permeability (only for anisotropic permeability), k_h is the horizontal permeability. According to Eq. 1, the smaller the standpipe cross-sectional area the faster the equalization occurs, because small volumes of water move to or from the standpipe.

k_h in Eq. 1 was evaluated by carrying out field tests (Hvorslev 1951) at variable head and solving the equation:

$$\ln \left(\frac{H(0)}{H(t)} \right) = \frac{F \cdot k_h}{A} \cdot t = m_h \cdot t \tag{2}$$

where, $H(0)$ and $H(t)$ are the active heads at time 0 and at any recorded time t , m_h is the coefficient estimated by linear regression. Given the values of m_h , the webGIS calculates automatically F , k_h and t_{95} for open-standpipe piezometers by using the relations:

$$F = \begin{cases} \frac{2\pi L}{\ln\left[\frac{mL}{D} + \sqrt{1 + \left(\frac{mL}{D}\right)^2}\right]}, & \text{if } \frac{mL}{D} \leq 4 \\ \frac{2\pi L}{\ln\left[\frac{2mL}{D}\right]}, & \text{if } \frac{mL}{D} > 4 \end{cases} \quad \text{with } m = \sqrt{k_h/k_v} \quad (3)$$

$$k_h = \frac{m_h \cdot A}{F} \quad (4)$$

$$t_{95} = -\frac{1}{m_h} \ln 0.05 \quad (5)$$

Input data and results are displayed in tables similar to that shown in Fig. 7. For filters located above the water table (piezometers “a”), it was not possible to carry out in situ permeability tests accordingly to Hvorslev (1951); in these cases, m_h was assigned instead of estimated from in situ permeability tests, and an unrealistic value of -99 for the square of the coefficient correlation was given to highlight this fact. In order to analyze in real time the effects of changes of filter size, pipe diameter, permeability anisotropy or hydraulic conductivity (gray cells in Fig. 7), the user may modify temporarily those values by clicking on the cells.

Due to the soil heterogeneity, different values of horizontal permeability, ranging between 10^{-7} and 10^{-4} m/s were estimated with the in situ permeability tests. Consequently, the time lags vary from some minutes to longer than a day, making them too different and too long to use those piezometers for monitoring the pore-water pressures in the soils.

For the automatic monitoring, the time lags were therefore reduced to a minimum value by lowering retrievable pressure transducers in the pipes and sealing the top of the filter tips. In this way, no volume of water has to move from or to the standpipe, but only an infinitely small volume of water is required to activate the sensor diaphragm (Dunnicliff 1993) and time lag reduces to some seconds (Penman 1961). Thus, the instruments obtained a very good conformance.

The multipoint extensometers have steel rods with plastic protective tubing, and anchors installed by using packers of geotextile and inflated with cement through injection tubes (Fig. 8). The borehole was filled with a cement-bentonite mixture only when it did not close by itself. Thus, the conformance of these instruments mainly depends on the ability of the anchors and head to move together with the surrounding soil. The anchors were clearly fixed to the soil thanks to the inflation, but the movement of the top head could be affected by the stiffness of the protective tubing and grout. The top head was therefore made with a square concrete plate $120 \times 120 \times 30$ cm since, because of its weight, it may deform the plastic tubing and the cement-bentonite grout and follow the soil movements. No data were collected neither processed to analyze this aspect. Soil displacements occurring between each anchor and the top head have been measured with displacement transducers fixed to the top head and lying on the top of the rod. Similarly, the conformance of the extensor-inclinometers TRIVEC (Fig. 9) depends on the stiffness of the grout and connecting tube that should deform as the surrounding soil and let the measuring marks to move.

Fig. 6 Sketch of the piezometer installation

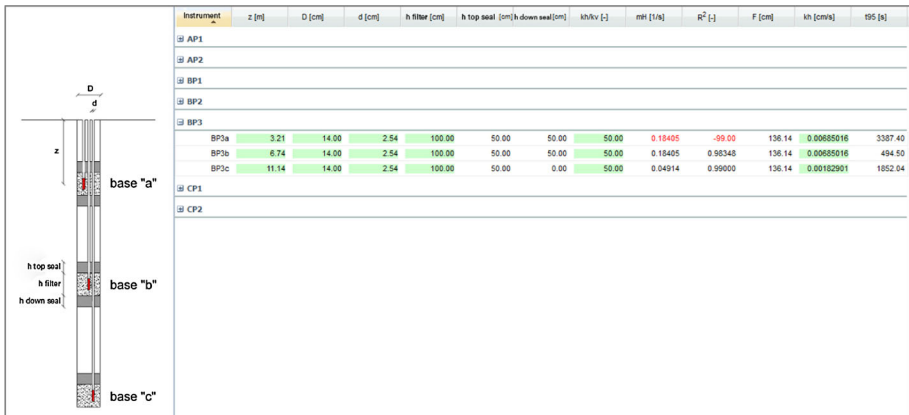
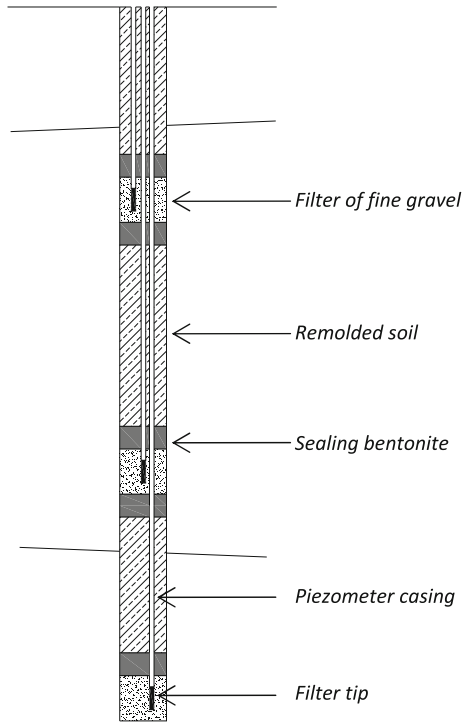


Fig. 7 Sketch (left window) and information (right window) of the piezometers displayed by the webGIS. Information are: input data (from left to right: z = depth of the pore-water pressure transducer, D = filter diameter, d = pipe diameter, h filter, h top seal; h lower seal; k_H/k_V = horizontal and vertical hydraulic conductivities ratio; mH = coefficient estimated by linear regression of permeability test data; R^2 = coefficient of determination of the linear regression) and results for the intake factor F, horizontal hydraulic conductivity k_H and time lag t_{95}

Fig. 8 Sketch of the extensometer installation

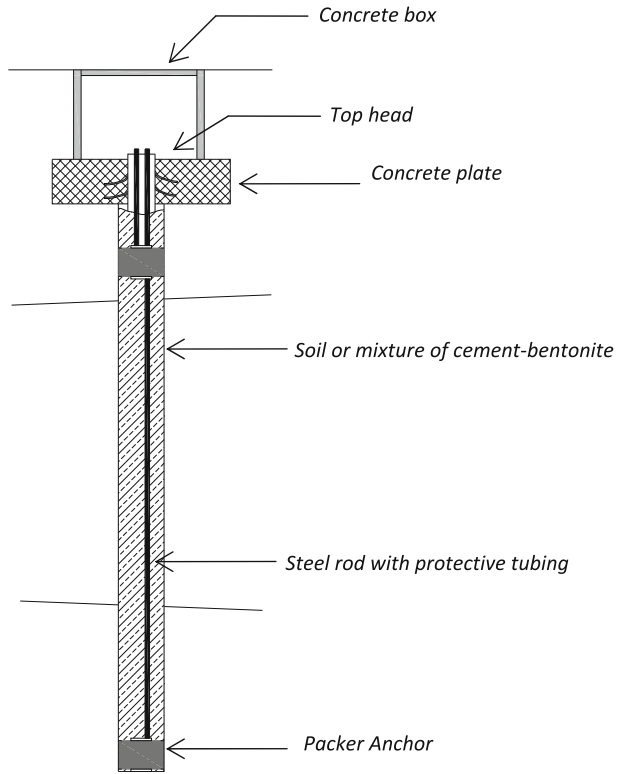
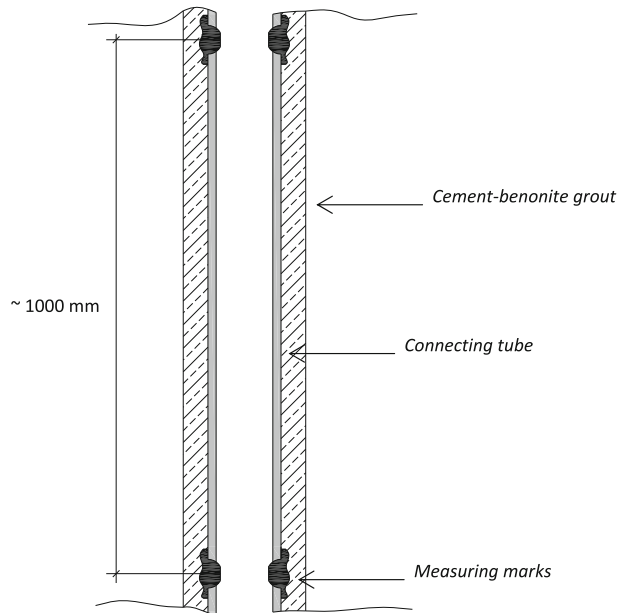


Fig. 9 Sketch of the extensor-inclinometer installation



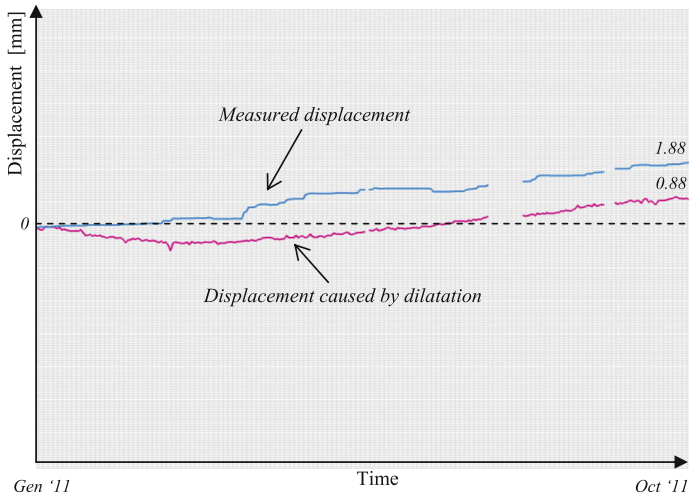


Fig. 10 Effect of rod dilatation on extensometer BMX2c displacement

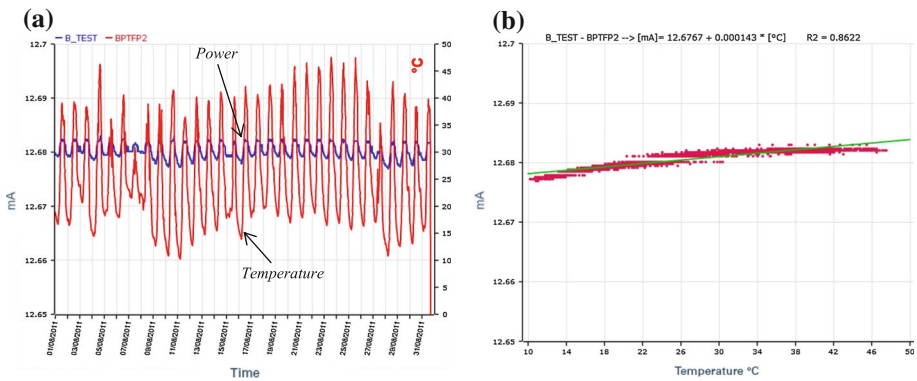


Fig. 11 Temperature effect on the AD conversion of datalogger B. **a** Recorded data of temperature and power of the stable signal of the card B versus time; **b** power of the stable signal versus temperature

6.2 Improper calibration

Calibration checks are required during the service life (Dunnicliff 1993). Thus, the webGIS offers tools by means of tables to calculate the deviation between an imposed value of the parameter (water pressure or displacement) and that calculated from the transducer signal by using the calibration curve. If the deviation is too large, the calibration of the transducer will be repeated and the new curve uploaded in the webGIS.

6.3 Temperature effects

Two kinds of temperature effects have been monitored: the effects of temperature on the dilatation of the steel rods of the extensometers and the effects on the analogical/digital conversion made by the datalogger. For this purpose, eight temperature sensors of PT100 type were installed in the box containing the datalogger of section B, in the top heads of

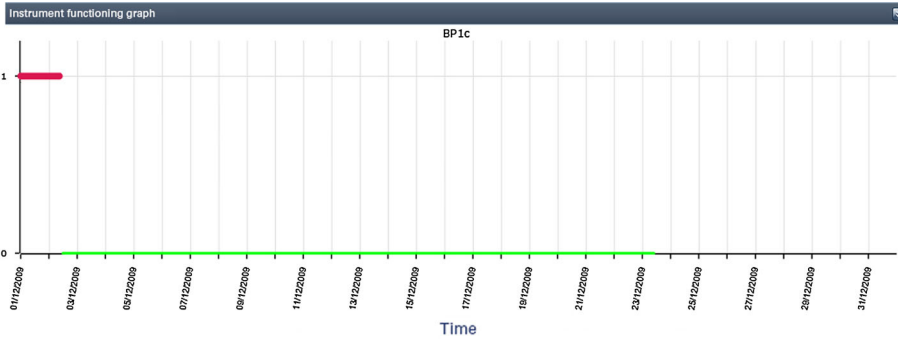


Fig. 12 Graph showing the functioning of piezometer BP1b: 1 = over-range signal (red color)

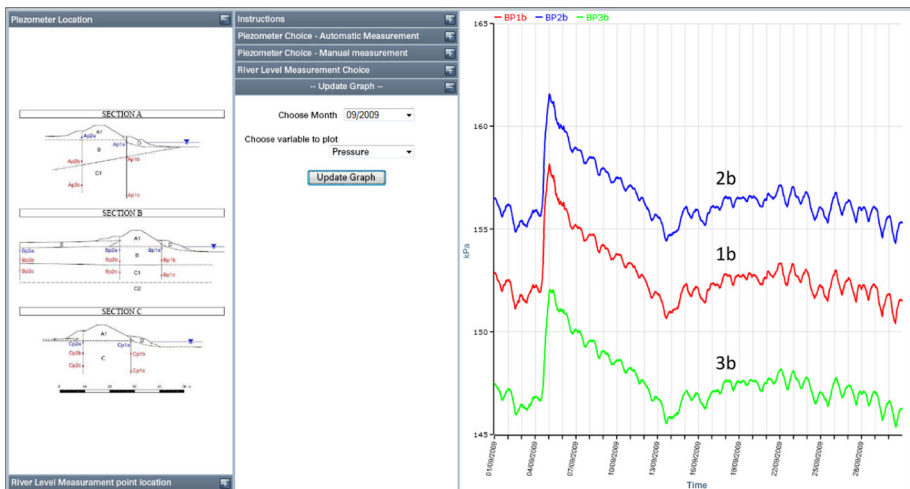


Fig. 13 Redundancy of piezometer measurements in terms of absolute pore-water pressure. *Left* sketch with the location of piezometers in the three sections A, B and C. *Central* boxes for entering the time (mm/yyyy) and the variable (absolute pressure or hydraulic head) to be plotted. *Right* absolute pressure versus time for piezometers BP1b, BP2b and BP3b

extensometers BMX1, BMX2 and BMX3, and at depths of 0.72, 2.52, 8.52 and 38.52 m from the top of BMX2.

To a first approximation, the webGIS calculates the dilatation of the steel rods at any time t by assigning to each reach of the rod the average value of temperature measured at the two ends and by assuming a coefficient of dilatation equal to $1.6 \times 10^{-5} \text{ }^\circ\text{C}^{-1}$. By seeing the example of graph shown in Fig. 10 for extensometer BMX2c, it is clear that almost the 50 % of the measured displacement is caused by the dilatation of the rod, thus this effect of temperature is not negligible and must be taken into account in the evaluation of the true soil vertical displacements.

Temperature may also influence the analogic/digital conversion and consequently vary the measures (Simeoni 2007). This effect of temperature was investigated at Egna by connecting three special cards to the dataloggers at sections A, B and C. The cards were

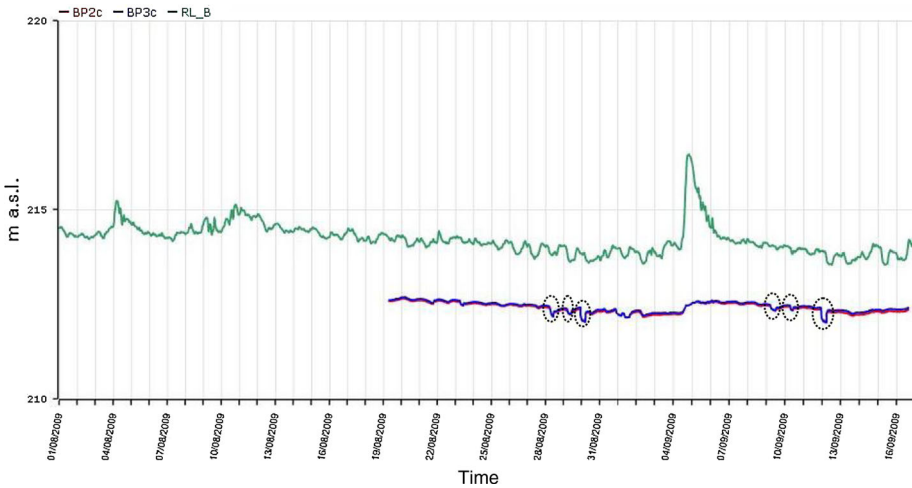


Fig. 14 Coherence of piezometer BP2c and BP3c measurements in terms of hydraulic heads and river level [m a.s.l.]

made in the laboratory to provide a constant power of about 13 mA. The webGIS displays in a graph the values of power and the measures of temperature at the datalogger B, and calculates the dependence of the signal on the temperature by a least-squares linear regression (Fig. 11). So far, the coefficients have varied between 1×10^{-4} and 5×10^{-4} mA/ °C, making the effect of temperature on the AD conversion negligible also for a maximum temperature change of 50 °C.

7 Data validation

Data validation has been carried out by comparing the measurements to the Full Scale and by analyzing their redundancy and coherence. The redundancy of measurements was analyzed by comparing measurements of the same type (processed in engineering units), while coherence was analyzed by comparing measurements describing the same physical phenomenon (Simeoni et al. 2008).

7.1 Comparison to the Full Scale

Almost all the measurements are given in the range 4–20 mA, except temperatures. For the 4–20 mA measurements, the webGIS checks if they are inside or outside the bounds and provides graphs with the signal versus time. Figure 12 shows an example of instrument functioning: value 1 (red line) means that the measure was over-range all the day, otherwise, it is 0 (green line). The signal would be 1 and yellow if the measure was over-range for less than a day.

7.2 Redundancy of measurements

For the piezometers, the user may decide which absolute water pressures the webGIS has to display. Figure 13 shows the absolute pore-water pressure measured in piezometers

BP1b, BP2b and BP3b. The three piezometers lie in soil B (ancient river bed) that has high permeability; accordingly the pressure changes were similar in the three piezometers and pressure decreased from the river (piezometers BP1b and BP2b) to the far field (piezometer BP3b).

The redundancy of the measurements of vertical displacement was analyzed by comparing the automatic measurements by extensometers to the manual ones carried out using TRIVEC.

7.3 Coherence of measurements

Coherence of piezometer measurements was analyzed by comparing the hydraulic heads and hydraulic gradients to the river level. In Fig. 14, the hydraulic head at piezometers BP2c and BP3c (almost the same) are compared to the river level. The piezometers lie in soil C1 that is less permeable than soil B. In fact, it has been observed that the hydraulic heads changed more slowly than the river level, since they did not display the daily oscillation. From August 19, 2009, the hydraulic heads were decreasing according to the average river level and increased on September 4, when a small flood was recorded. In the

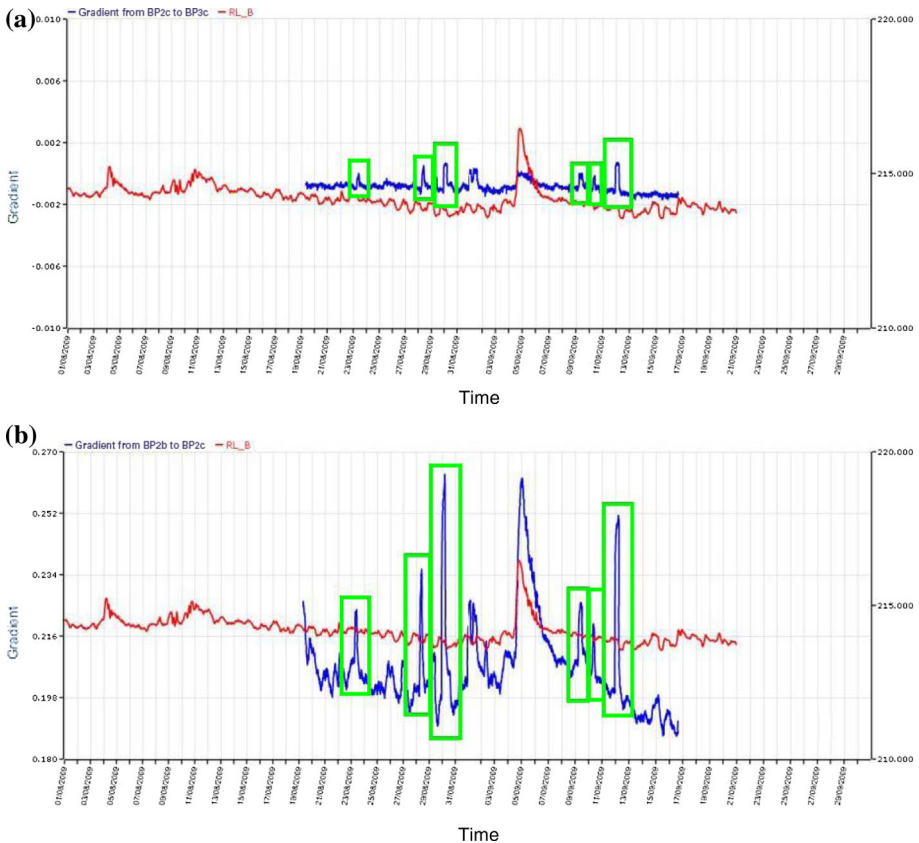


Fig. 15 Coherence of piezometer measurements in terms of hydraulic gradients and river level [m a.s.l.]. **a** Hydraulic gradient from BP2c to BP3c; **b** hydraulic gradient from BP2b to BP2c

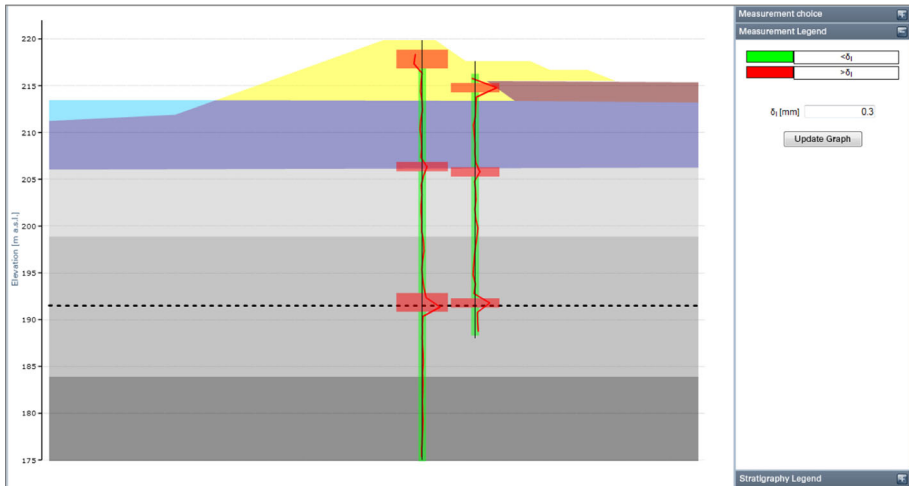


Fig. 16 Coherence of extensometer measurements by TRIVEC compared to soil profile. *Right Box* for entering the vertical displacement threshold δ_1 (in this example $\delta_1 = 0.3$ mm was selected); *left* interval depths where vertical displacements resulted higher than δ_1 are automatically displayed in *red* and with larger hatched areas

same figure, it should be noted that on August 23, 28, 30 and September 9, 10, 12 the hydraulic head in piezometers BP2c and BP3c showed sharp decrements. The reliability of these measurements was analyzed in terms of hydraulic gradient. Figure 15 shows the average hydraulic gradient, calculated as the hydraulic head difference over the distance, from piezometer BP2c to piezometer BP3c (Fig. 15a) and from BP2b to BP2c (Fig. 15b). On those days, the hydraulic gradients showed sharp increments revealing water seepage toward the field, from BP2c to BP3c, and downwards, from BP2b to BP2c. This phenomenon could be explained with the water extraction for irrigating the apple orchards.

Finally, the coherence of the manual extensometer measurements by TRIVEC was analyzed by comparing the local vertical displacements to the soil profile (Fig. 16). Displacements larger than a threshold $\delta_1 = 0.3$ mm occurred at depths where peat layers were identified in the soil profile, and therefore, where a secondary consolidation process may take place.

8 Conclusions

The current system, combining a spatial DBMS and a webGIS, has proved to be a suitable tool for fast and standardized operations for managing and analyzing data describing a monitoring site.

In particular, there are clear advantages for the management of data describing the instruments, such as geometry, features and calibration functions, as well as for analyzing their conformance. At the same time, the same tool can be used for data validation in terms of signal range, coherence and redundancy, thus it is possible to identify faults and a real-time check of the compliance of the system as a whole is possible.

Most of the user of the system benefits from the possibility of data processing and data visualization in a quick and flexible way, using a standard and remote client.

During its operation, the system was fundamental in detecting the non-functioning status of defective instruments as soon the relevant data were uploaded. The data analyses automatically performed by the system pointed out the absence of redundancy for the vertical displacement measurements (by comparing manual measurements to automatic measurements) and the environmental effects on the displacement measurements (temperature change).

On the other hand, the coherence between pore-water pressure measurements and seepage due to river level changes was verified, as well as the coherence between vertical displacement measurements and secondary consolidation due to the presence of peat layers.

The database and the webGIS facilitated the data management for the seepage and stability analysis, as well as the data sharing among research groups and public administrations. The Adige River embankment was selected by the Research Training Network European Project MUSE (“Mechanics of Unsaturated Soils for Engineering,” <http://muse.dur.ac.uk/>) as a case study to provide benchmarking of constitutive and numerical modeling capabilities for unsaturated soils. For example, Pozzato (2009) used the piezometer measurements to estimate the horizontal and vertical hydraulic conductivities by carrying out inverse analyses of the flow process in the foundation layers. Once the hydraulic model of the levee (mainly soils above the water table) and its foundation (soils below the water table) was defined, the pore-water pressure buildups during four historical flood events were simulated, revealing that the water flow at the outer toe of the embankment may have a significant upward component. Thus, failure mechanisms due to outer slope failure were assumed to be likely to occur for this embankment.

Acknowledgments The work has been partially supported by the Autonomous Province of Bolzano-Bozen, Italy, that funded for the field instrumentation. The authors are grateful to Mr Davide Ronco for his contribution to prepare the images from the webGIS.

References

- Cho SE (2012) Probabilistic analysis of seepage that considers the spatial variability of permeability for an embankment on soil foundation. *Eng Geol* 133–134:30–39
- Christian JT, Ladd CC, Baecher GB (1994) Reliability applied to slope stability analysis. *J Geotech Eng* 120(12):2180–2207
- Crossland MD, Wynne BE, Perkins WC (1995) Spatial decision support systems: an overview of technology and a test of efficacy. *Decis Support Syst* 14(3):219–235
- DiBiagio E, Kjekstad O (2007) Early warning, instrumentation and monitoring landslides. In: Proceedings of the 2nd regional training course, RECLAIM II, 29th January–3rd February 2007
- Dunnicliff J (1993) *Geotechnical instrumentation for monitoring field performance*, new ed. Wiley, New York
- Elkateb T, Chalaturnyk R, Robertson PK (2003) An overview of soil heterogeneity: quantification and implications on geotechnical field problems. *Can Geotech J* 40(1):1–15
- Ext JS Cross-Browser Rich Internet Application Framework (2010) <http://www.sencha.com/products/js/>. Accessed 12 Dec 2010
- Fan-Chieh Y, Chien-Yuan C, Sheng-Chi L, Yu-Ching L, Shang-Yu W, Kei-Wai C (2007) A web-based decision support system for slopeland hazard warning. *Environ Monit Assess* 127(1–3):419–428
- Gallage C, Uchimora T (2010) Investigation on parameters used in warning systems for rain-induced embankment instability. In: Proceedings of the 63rd Canadian geotechnical conference (GEO2010), GEO2010 Calgary, Calgary, Alberta, pp 1025–1031
- GeoServer website (2010) <http://geoserver.org>. Accessed 12 Dec 2010
- Gui S, Zhang R, Turner JP, Xue X (2000) Probabilistic slope stability analysis with stochastic soil hydraulic conductivity. *J Geotech Geoenviron Eng* 126(1):1–9

- Hopman V, Kruiver P, Koelewijn A, Peters T (2011) How to create a smart levee. In: Proceedings of the 8th international symposium on field measurements in GeoMechanics 2011, Berlin, Germany, September 12–16
- Huang P, Yao J-G, Lu L, Jin A, Wei L (2005) Design of WebGIS based power quality monitoring system and its application. *Power System Technol* 29(7):52–55
- Hvorslev MJ (1951) Time lag and soil permeability in ground-water observation. Bulletin No. 36, Waterways Experiment Station, Corps of Engineers, U.S. Army, Vicksburg, Mississippi, pp 50
- MapFish website (2010) <http://mapfish.org>. Accessed 12 Dec 2010
- Marr WA (2013) Instrumentation and monitoring of slope stability. In: Proceedings of the Geo-Congress 2013, ASCE, stability and performance of slopes and embankments III, San Diego (CA, USA), 3–6 March 2013, pp 2224–2245
- Marsland A, Randolph MF (1978) A study of the variation and effects of water pressures in the pervious strata underlying Crayford Marshes. *Geotechnique* 28(4):435–464
- Meijer RJ, Koelewijn AR (2008) The development of an early warning system for dike failure. In: Proceedings of the 1st international conference and exhibition on waterside security 2008, August 26–28, 2008, Copenhagen, Denmark
- Merz B (2006) Abschätzung von Hochwasserrisiken. Methoden, Grenzen und Möglichkeiten, Habilitationsschrift, E. Schweizerbart'sche Verlagsbuchhandlung (Nägele und Obermiller), Stuttgart, Germany
- Morris MW, Allsop W, Buijs FA, Kortenhuis A, Doorn N, Lesniewska D (2009) Failure modes and mechanisms for flood defence structures. In: Samuels P, Huntington S, Allsop W, Harrop J (eds) Flood risk management: research and practice. Taylor & Francis Group, London, pp 693–701
- Norwegian Geotechnical Institute (NGI) (2000) Ralph B. Peck: Engineer, educator, a man of judgment. In: DiBiagio E, Flaate K (eds) Publication 207, NGI, Oslo, Norway
- Oka F, Kimoto S, Kato R, Sunami S, Kodaka T (2008) A soil-water coupled analysis of the deformation of an unsaturated river embankment due to seepage flow and overflow. In: Proceedings of the 12th international conference of IACMAG 2008, 1–6 October 2008, Goa, India, pp 2029–2041
- Open Flash Chart project (2010) <http://teethgrinder.co.uk/open-flash-chart/HYPERLINK> “<http://teethgrinder.co.uk/open-flash-chart/>”. Accessed 12 Dec 2010
- Open GIS Consortium Inc. website (2010) <http://www.opengeospatial.org/>. Accessed 18 May 2010
- OpenLayers: Free Maps for the Web (2010) <http://openlayers.org>. Accessed 12 Dec 2010
- Penman ADM (1961) A study of the response time of various types of piezometer. In: Proceedings of the conference on pore pressure and suction in soils 1961, London, Butterworths, pp 53–58
- PostGIS website (2010) <http://postgis.refractory.net>. Accessed 12 Dec 2010
- PostgreSQL website (2010) <http://www.postgresql.org>. Accessed 12 Dec 2010
- Pozzato A (2009) Stability of river embankment of coarse-grained well graded soil: the case study of the Adige river at Egna (BZ), Ph.D. Thesis, University of Trento
- Simeoni L (2007) Laboratory and in situ tests on an automatic monitoring system with IPIs. In: Proceedings of the 7th international symposium on field measurements in geomechanics 2007, Boston, USA, 24–27 September 2007, ASCE Geotechnical Special Publication 175
- Simeoni L, Tarantino A, Pozzato A, De Polo F, Bragagna M (2008) The design of a monitoring system for an embankment of the Adige River. *Italian Geotech J* 42(3):73–94 (in Italian)
- Staiano T, Rinaldi M, Paris E (2001) Seepage and stability analysis of embankments during flood events. In: Proceedings of the XXIX IAHR congress, 21st century: new era for hydraulic research and its application 2001, Beijing, 16–21 September 2001
- The Apache Software Foundation (2010) <http://www.apache.org>. Accessed 12 Dec 2010
- Van Beek VM, de Bruijn HTJ, Knoeff JG, Bezuijen A, Förster U (2010) Levee failure due to piping: a full scale experiment. In: Burns SE, Bhatia SK, Avila CMC, Hunt BE (eds) Proceedings of the 5th international conference on scour and erosion ICSE5 2010. ASCE Geotechnical Special Publication no. 210, pp 283–292
- Van Der Most H, Wehrung M (2005) Dealing with uncertainties in flood risk assessment of dike rings in the Netherlands. *Nat Hazards* 36:191–206
- Vaughan PR (1969) A note on sealing piezometers in boreholes. *Géotechnique* 19(3):405–413
- Vorogushyn S, Merz B, Apel H (2009) Development of dike fragility curves for piping and micro-instability breach mechanisms. *Nat Hazards Earth Syst Sci* 9:1383–1401
- Vrijling JK (2001) Probabilistic design of water defence systems in The Netherlands. *Reliab Eng Syst Saf* 74:337–344
- Werth K (2003) Geschichte der Etsch. Tappeiner Verlag, Lana (BZ)
- Yoo C, Kim J-M (2007) Tunneling performance prediction using an integrated GIS and neural network. *Comput Geotech* 34:19–30